Theoretical and experimental studies of copper(II) and nickel(II) complexes derived from the ligand *N*-benzyl benzimidazole as corrosion inhibitors in ionic and bacterial media

Maab Khattab Omer,[1] Abeer A. Ibrahim,[2] Rafah Mohammed Thyab,[3] M.M. Kadhim,[4,5]* A.W. Salman[6] and Mohammed Ali Yaseen[7]

[1]*Chemistry Department, College of Science for Women, University of Baghdad, 34004, Baghdad, Iraq*
[2]*Anesthesia Department, Health & Medical technical colleges, Al-ayen university, Al Nasiriya, 64001, Iraq*
[3]*University of Kufa, College of science, Department of chemistry, 54001 Najaf, Kufa Street, Iraq*
[4]*College of dentistry, Islamic University, 54001 Najaf, Kufa Street, Iraq*
[5]*Department of Medical Laboratory Techniques, Dijlah University College, Baghdad, 10021, Iraq*
[6]*Department of Production, College of Agriculture, Wasit University, Kut, Wasit, 52001, Iraq*
[7]*Medical Laboratories Techniques Department, Al-Mustaqbal University College, Babylon, Hilla, 51001, Iraq*
**E-mail: Mustafa_kut88@yahoo.com*

Abstract

The current study discusses the possibility of using dinitrobis(*N*-benzyl benzimidazole) copper(II) (Alpha-Cu and Beta-Cu) and dichlorobis(*N*-benzyl benzimidazole) nickel(II) (Ni) complexes as corrosion inhibitors using Density Function Theory (DFT). The research proposed using the above-mentioned complexes to inhibit the corrosion induced by aggressive ions and/or *Acidithiobacillus ferrooxidans* bacteria (*A. ferrooxidans*). Total Electron Density (TED) and Mulliken charges were calculated to determine the adsorption active sites on the studied molecules. HOMO, LUMO, dipole moment, energy gap, and other characteristics were also employed to compare the efficiency of the proposed inhibitors by Gaussian 09 program. Docking calculations were utilized to assess the inhibition of *A. ferrooxidans* based on binding energy (E_b). DFT results indicated that both complexes have good inhibition efficiency according to the studied parameters and adsorption properties in both media. Further, an experimental part was included to supplement the theoretical one, using the polarization method at 10 ppm and 35°C. The order of efficiency was Alpha-Cu > Beta-Cu > Ni according to the theoretical and experimental parts.

Received: February 14, 2022. Published: April 21, 2022 doi: 10.17675/2305-6894-2022-11-2-12

Keywords: *DFT, benzimidazole, adsorption, corrosion, docking.*

1. Introduction

Corrosion is a natural phenomenon, in which the metal is converted into more stable (less energy) compounds such as oxides, hydroxides, sulfides, or carbonates. This process can be done by chemical and/or electrochemical reactions of the metals with their environment. One of the most important metals is iron or steel, which react with oxygen and water in the environment to form hydrated iron oxides, also known as rust, which is chemically identical to the original ore composition [1–4].

Corrosion is easy to be seen on chemical and petrochemical equipment, which is one of the biggest problems in this industry. To prevent or decrease corrosion, different techniques, such as coating, cathodic protection, and corrosion inhibitors, have been utilized [5–7]. Corrosion inhibitors are chemicals with different chemical structures and inhibition mechanisms that significantly reduce corrosion rates when used in small amounts.

Inorganic inhibitors are widely used because of their high performance and ease of synthesis. Most vitamin B complexes, dyes, enzymes, antibiotics, alkaloids, amino acids, and drugs contain heterocyclic compounds with substituents other than carbon. The five-membered oxadiazole is highly reliable for various industrial applications [8–13]. Inorganic compounds are found to have a significant advantage in corrosion inhibition, which was due to their role in limiting corrosion under various corrosive conditions. A protective coating is produced on the metal surface, and these molecules are particularly efficient in preventing corrosion caused by water.

Ligands that contain heteroatoms such as phosphorus, sulfur, nitrogen, and oxygen are found in most known inorganic inhibitors. One or more functional groups containing one or more heteroatoms are commonly found in potent organic inhibitors [4, 5, 15].

Depending on the active sites, the inhibition efficiency is related to O, N, S, and P atoms. In an acidic medium, S and N-containing inhibitors are commonly used. Furthermore, compared to molecules containing only one of these heteroatoms, molecules containing nitrogen and sulfur can afford an excellent inhibition efficiency [16]. The electron density and polarizability of the functional group determine the strength of the adsorption bond [17]. The current research aims to investigate the corrosion inhibition efficiency of two metal complexes, dinitrobis(*N*-benzyl benzimidazole)copper(II), and dichlorobis(*N*-benzyl benzimidazole)nickel(II) [18], using density functional theory principles (DFT). In both complexes, the central metal ion is coordinated with two moieties of *N*-benzyl benzimidazole and two chloride ions in the case of Ni(II) complex, and two nitrate ions in the case of Cu(II) complex. The theoretical inhibition efficiency is directly correlated to some quantum chemical parameters dealt with in the current study. Last but not least, docking calculations are also used to investigate the possibility of corrosion inhibition caused by specific microorganisms.

2. Calculations models

The current study employed three software applications. A hybrid function of Becke three-parameters Lee, Yang, and Parr were used in the quantum chemical computations (B3LYP) by Gaussian 09. In addition, to correct electrical characteristics and geometries for complexes, the LanL2DZ basis set produces equivalent findings [19, 20], which was done in a vacuum [21–23]. The docking calculations were performed using the Molecular Graphics Laboratory (MGL). The program simulated protein–ligand interactions as well as other biomolecular systems. These simulations predicted the involvement of the studied compounds in inhibiting bacterial corrosion. The bacteria *Acidithiobacillus ferrooxidans* was chosen for its corrosive effect and iron atom dissolution [24]. The selected bacteria's protein structure (3f9s) was retrieved from RCSB [25]. The ADT tool in Molecular Graphics Laboratory was used to evaluate the structures of both the protein and the inhibitors [26]. The Autodock was performed by the Discovery Studio Visualizer (DSV) program [25] to determine the molecule's root.

3. Results and Discussion

3.1. Inhibition parameters

We employed the LanL2DZ basis set, which gives natural electrical characteristics and geometries for complicated structures in the ground state (Figure 1) [27]. The cupper element is considered with electrons in two directions (alpha and beta). The calculations were made in a vacuum [28, 29]. Limit orbital theory was used to predict the inhibitor-metal surface interaction [30]. The FMO provides significant evidence for stability via the difference in orbital energy as $E=E_{LUMO}-E_{HOMO}$. High E_{HOMO} values of the inhibitor molecule suggest a predisposition for giving electrons. The ability of a molecule to receive an electron is measured by its LUMO energy (E_{LUMO}). The energy gap ($E=E_{LUMO}-E_{HOMO}$), dipole moment (μ), electronegativity (χ), ionization potential (*IP*), electron affinity (*EA*), and global softness (*S*) are all connected to the inhibitory efficiency of the examined compounds (Table 1 and Table 2). The inhibitor's effectiveness improves when the energy gap between orbital borders (*E*) decreases [31].

Koopman's [32] theory links the ionization potential and electron affinity to negative HOMO and LUMO energies. The ionization potential of a neutral atom is the energy required to remove one electron. The low ionization energy indicates a good efficiency of the studied inhibitor. Electron affinity (*EA*) is the energy generated by a neutral atom upon gaining an electron. The less stable system is the more efficient the inhibition. Hardness (η) is the second derivative of *E*, which measures both stability and reactivity [33]. Electronegativity is an atom's capacity to pull shared electrons to its side. Low electronegativity suggests a significant efficiency of the inhibitor. *S* refers to the inverse of global hardness (η), which determines the stability and reactivity of molecules [34]. Parr's global electrophilicity index (χ) measures a molecule's stabilization energy after receiving more electrons. Good inhibitors have a low global electrophilicity index. Figure 2 compares

the best inhibitors depending on the measured parameters. The studied parameters were calculated using equations (1–6):

$$IP = -E_{\text{HOMO}} \tag{1}$$

$$EA = -E_{\text{LUMO}} \tag{2}$$

$$\omega = \frac{(-X)^2}{2\eta} \tag{3}$$

$$S = \frac{1}{\eta} \tag{4}$$

$$\eta = \frac{IP - EA}{2} \tag{5}$$

$$\chi = \frac{IP + EA}{2} \tag{6}$$

Figure 3 compares the studied parameters of the studied complexes. Depending on the results of E_{HOMO}, E_{LUMO}, ΔE, μ, *IE*, *EA*, χ, η, *S* and ω parameters, all the studied complexes could be used as inhibitors, and the order of efficiency was Alpha-Cu > Beta-Cu > Ni.

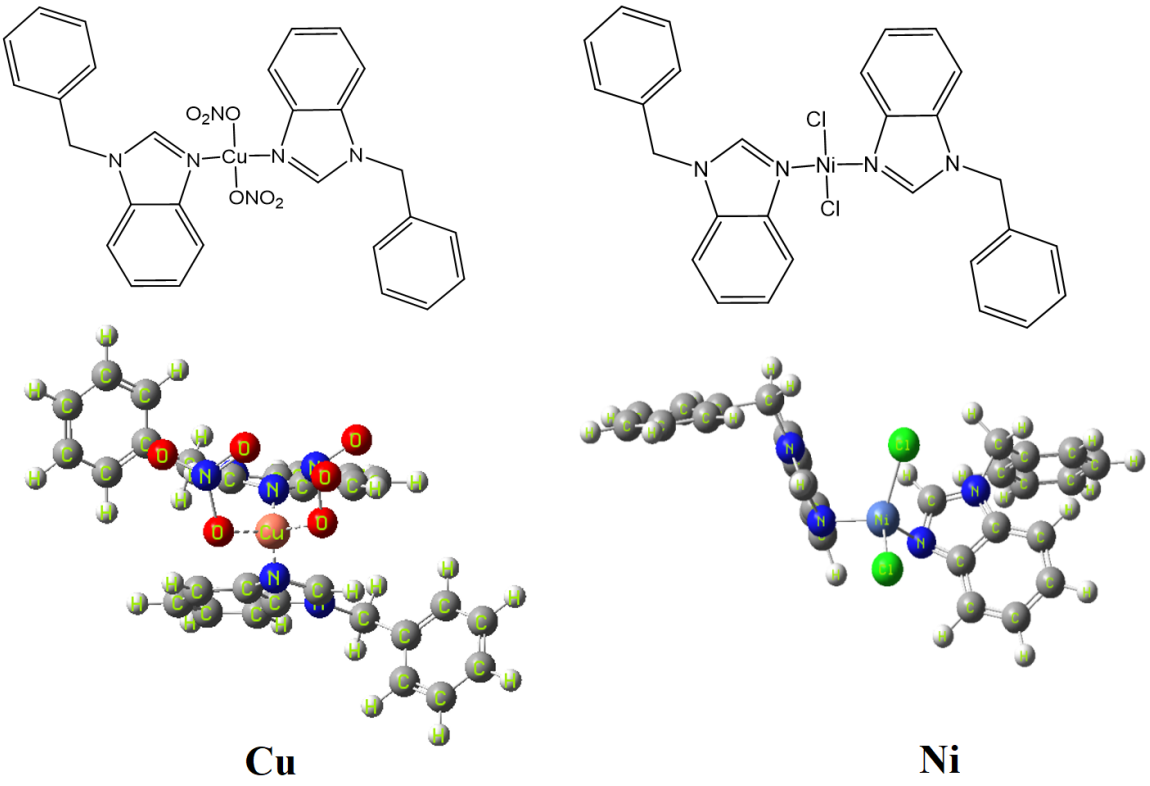

Figure 1. Optimized structures of Ni and Cu complexes.

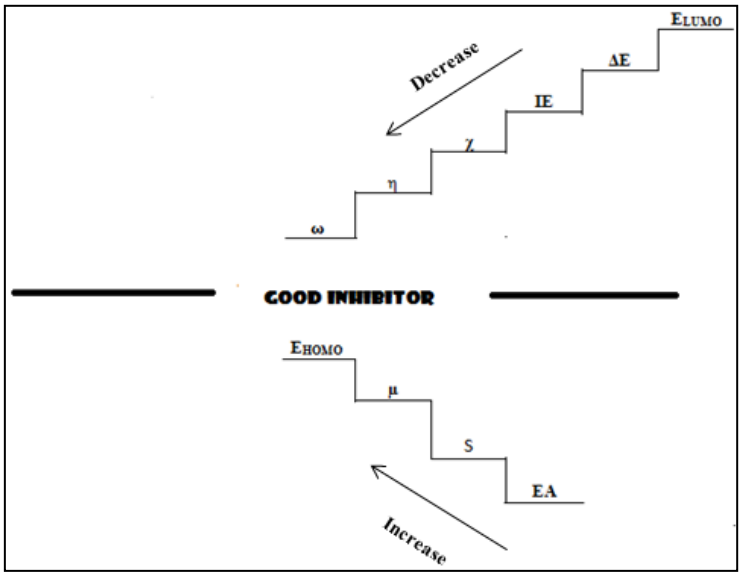

Figure 2. The relationship of inhibitors with the studied parameters.

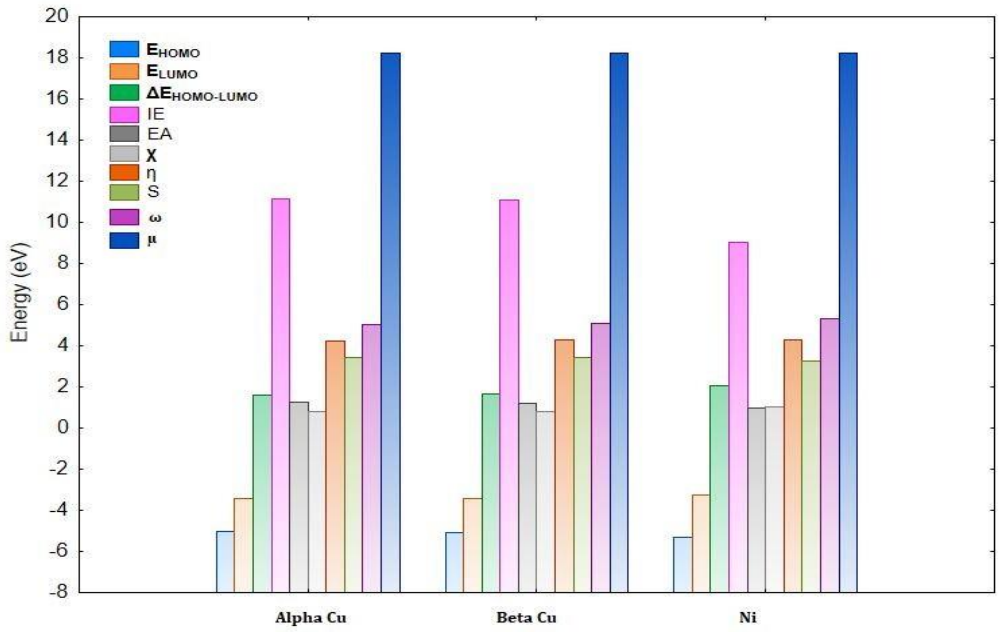

Figure 3. Comparison of studied parameters of the studied complexes.

Table 1. DFT estimated characteristics of inhibitor molecules in vacuum at equilibrium geometries.

Inhibitors	E_{HOMO} **(eV)**	E_{LUMO} **(eV)**	$\Delta E_{HOMO-LUMO}$ **(eV)**	**μ (Debye)**
Alpha-Cu	–5.025	–3.422	1.603	18.244
Beta-Cu	–5.094	–3.450	1.644	18.244
Ni	–5.313	–3.277	2.0362	9.250

Table 2. DFT computed parameters for inhibitor molecules in vacuum.

Inhibitors	*IE* (eV)	*EA* (eV)	χ (eV)	η (eV)	*S* (eV)	ω (eV)
Alpha-Cu	5.025	3.422	4.223	0.801	1.247	11.126
Beta-Cu	5.094	3.450	4.272	0.822	1.2162	11.101
Ni	5.313	3.277	4.295	1.018	0.982	9.062

3.2. Molecule Orbitals (HOMO-LUMO)

Figure 4 shows the geometries optimization of investigated compounds in the gas phase, including LUMO and HOMO density distributions. Red refers to high electron density, whereas green shows low electron density [37]. The high electron density area donates electrons to the metal surface, whereas the low electron density area accepts electrons [38]. So the location of these two sectors is crucial. Cu-complex possesses a high electron density near the receptor site, which is facilitated by oxygen atoms and double bonds. While the Ni-complex appears to be equivalent in terms of receptors and donors, since Cl, O, and Ni are all active sites.

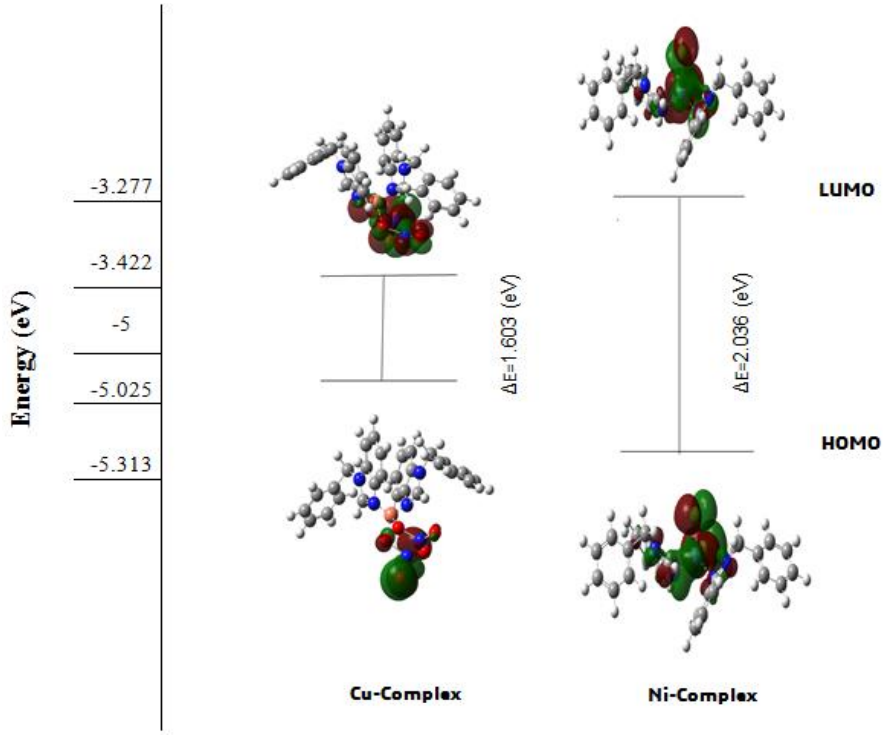

Figure 4. Orbital density distributions of studied complexes.

3.3. Adsorption sites

The electron density of the donor atom affects the strength of the adsorption bond. Total electron density (TED) is referring to the electron density of a molecule. In Figure 5, the O, N, and Cl atoms and some parts of the double bond are highlighted in red, indicating potential

electrophilic attack sites. Whereas, the yellow highlighted areas have moderate electronegativity. The blue area is the optimum positive area for receiving electrons from the donors [39].

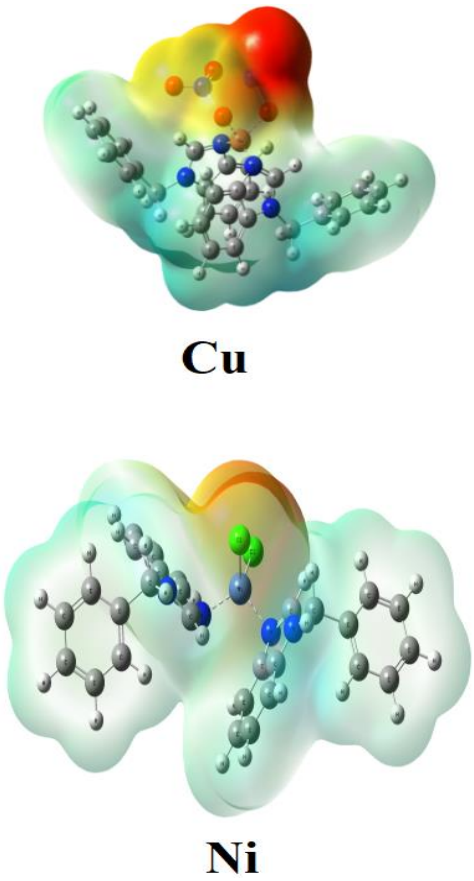

Figure 5. TED map of the studied complexes.

The local reactivity of complexes was investigated using the Mulliken charges population analysis (nucleophilic and electrophilic centers). As a result, high-charge molecule areas are softer than low-charge ones. So, while determining reactivity, the electron density is vital. Chemical adsorption, the interactions between the adsorbent and adsorbate can be electrons shared or orbitals.

Proven charges influence the physicochemical properties of compound reactions [40, 41]. As a result, the site of the nucleophilic attack will be where the positive charge value is most significant. The positive charge determines the electrophilic attack location. Thus, in the most reactive compound (Cu-complex), electrophilic attack prefers Cu, N, H, and C, while in the Ni-complex, it prefers N, C, and H. The green and red colors represent the positive and negative charges, respectively. The decrease in color intensity indicates a decrease in electrophilicity of nucleophilicity. The most reactive sites for the nucleophilic attack that can donate electrons to Cu and Ni complexes are found at the atoms O, C, and N for Cu-complex, and Ni, Cl, C, and N for Ni-complex (Figure 6).

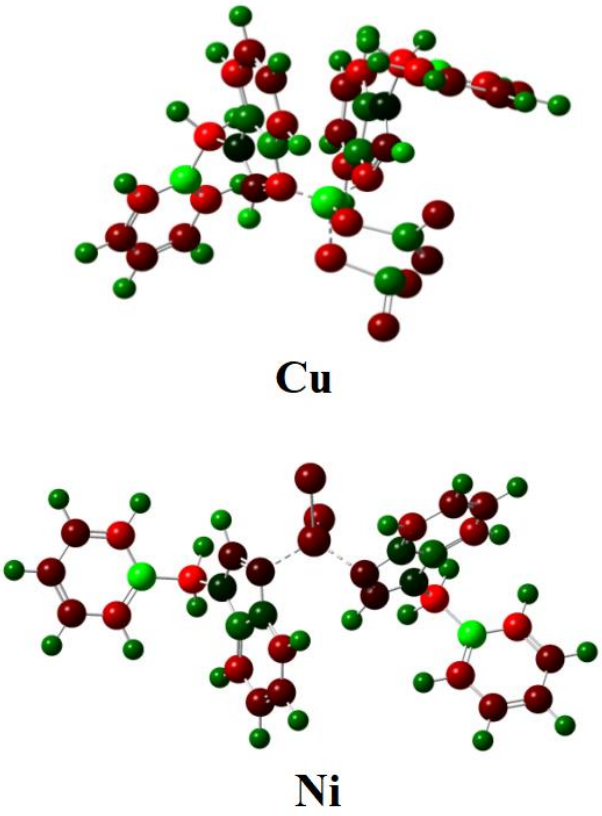

Figure 6. Mulliken charge of the studied complexes.

3.4. Docking studies

Docking studies estimate how a molecule will align with another when they are bonded together to create a stable complex. The binding or association affinity between two molecules can be predicted by their preferred orientation. The chosen complexes (Cu and Ni) were examined as inhibitors of the corrosive bacteria *Acidithiobacillus ferrooxidans* (*A. ferrooxidans*). Hydrogen ions, an electron receptor, induce the rusting caused by *A. ferrooxidans* [42].

Binding energy (E_b) reflects the affinity of complexes to the receptor, whereas ligand efficiency (L_E) is defined as the binding energy per atom of ligand for the receptor protein (Figure 7) [43, 44]. According to the E_b value, both Cu (E_b=−4.93 kcal/mol), and Ni (E_b=−7.43 kcal/mol) complexes are possible to hinder *A. ferrooxidans* bacteria (Table 3). The favored binding sites on the receptor are 1 for Cu-complex, and 9 for Ni-complex. In general, Ni complex showed inhibitory activity in bacterial media more than Cu complex.

Table 3. Binding energy and ligand efficiency of studied complexes.

Comp.	E_b (kcal/mol)	L_E	E_b range	Best site number
Cu	–4.93	–0.12	–2.49 to –4.93	1
Ni	–7.43	–0.21	–6.09 to –7.43	9

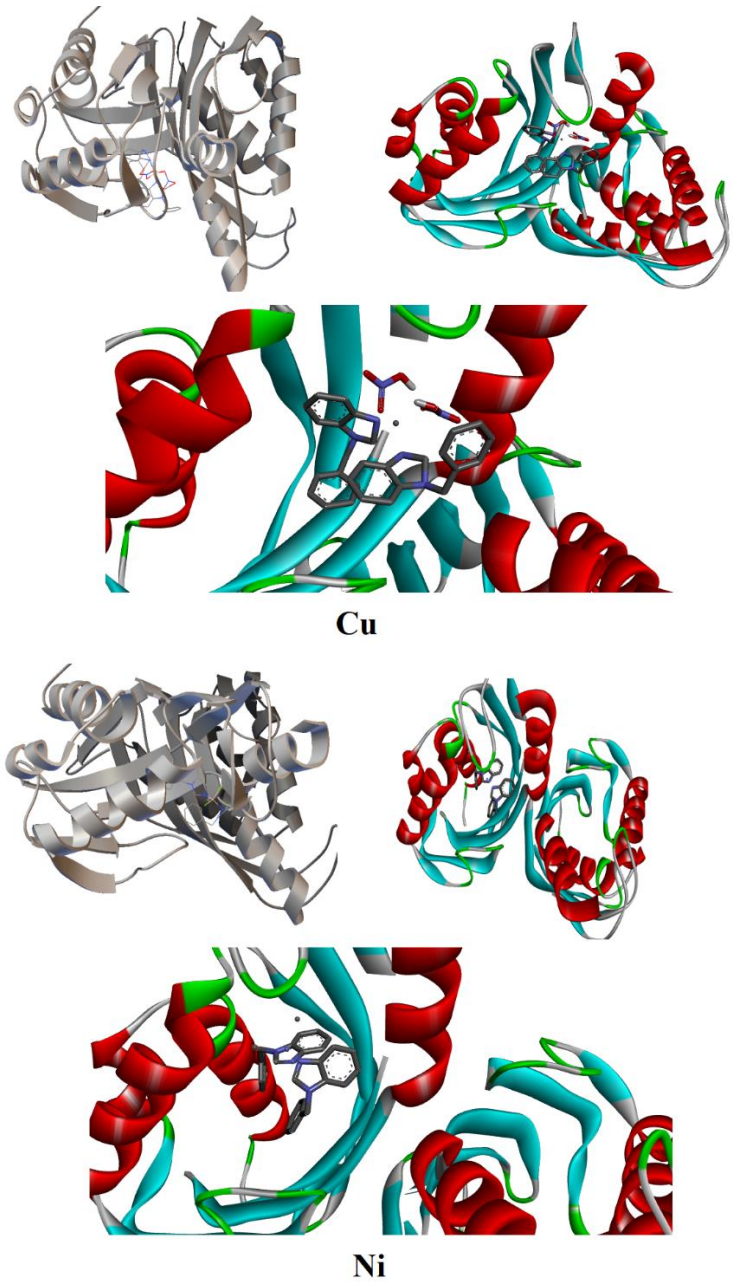

Figure 7. *A. ferrooxidans* receptor interactions with the complexes.

3.5. Experimentally confirmation

Inhibitors were prepared at a concentration of 10 ppm. The stainless steel was used as the protective alloy. At a controlled laboratory temperature, the inhibition efficiency was evaluated for the concentration at 35°C. The polarization curves were extrapolated using the extrapolation method. Table 4 shows the correlation between i_{corr} and inhibition efficiency %*IE*, which was calculated using the following equation:

$$\%IE = \frac{i_{corr}^{0} - i_{corr}}{i_{corr}^{0}} \cdot 100 \quad (7)$$

where i_{corr}^{0} and i_{corr} are the corrosion rate without and with inhibitors, respectively [41]. The corrosion medium used is HCl at 0.1 M. According to %*IE*, the inhibition efficiency of Cu-complex is larger than Ni-complex. The Scanning Electron Microscope (SEM) image showed that the inhibitor Cu-complex was distributed on the surface of the stainless steel used in the experiment (Figure 8).

Table 4. The current of corrosive media without and with inhibitors.

Inhibitors	i_{corr} **(μA·cm^{-2})**	***IE*%**	**Blank i_{corr} (μA·cm^{-2})**
Cu-complex	$5\cdot10^{2}$	88.3	$4.31\cdot10^{3}$
Ni-complex	$11\cdot10^{2}$	74.4	

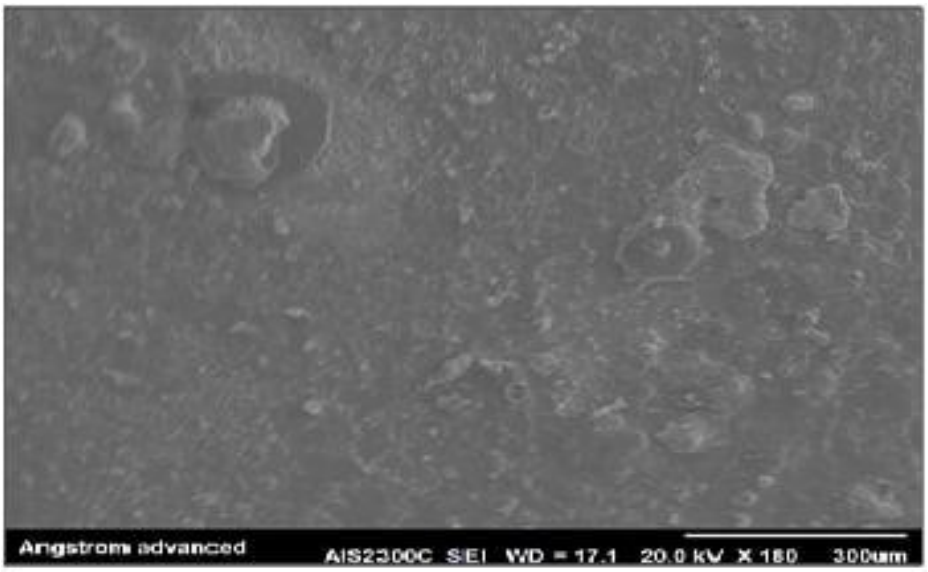

Figure 8. SEM image of Cu-complex on the stainless steel.

4. Conclusions

In the current study, the activity of Cu and Ni complexes in the ground state as corrosion inhibitors was investigated using DFT (B3LYP) computations using LanL2DZ. The efficiency of the studied inhibitors was investigated in both ionic and bacterial media. The results revealed an excellent inhibition efficiency for Cu-complex in the ionic medium, which was better than Ni-complex. While in bacterial medium, docking study revealed an excellent inhibition efficiency for Ni-complex, as it was better than Cu-complex. In general, DFT results indicated that the inhibition efficiency was good in both complexes according to the studied parameters and adsorption properties (TED and Mulliken charge). Finally, the polarization results proved that the Cu-complex (%*IE*=88.3%) is more active than the Ni-complex (%*IE*=74.4).

References

1. J.R. Davis, *Corrosion: understanding the basics*, 2000. doi: 10.5860/choice.37-6294
2. H.H. Krause, High temperature corrosion problems in waste incineration systems, *J. Mater. Energy Syst*., 1986, **7**, 322–332. doi: 10.1007/BF02833571
3. A.H. Radhi, E.AB. Du, F.A. Khazaal, Z.M. Abbas, O.H. Aljelawi, S.D. Hamadan, H.A. Almashhadani and M.M. Kadhim, HOMO-LUMO Energies and Geometrical Structures Effecton Corrosion Inhibition for Organic Compounds Predict by DFT and PM3 Methods, *NeuroQuantology*, 2020, **18**, no. 1, 37–45. doi: 10.14704/nq.2020.18.1.NQ20105
4. S.S. Prabha, R.J. Rathish, R. Dorothy, G. Brindha, M. Pandiarajan, A. Al-Hashem and S. Rajendran, Corrosion Problems in Petroleum Industry and their solution, *Eur. Chem. Bull*., 2014, **3**, 300–307.
5. R.M. Kubba and M.M. Khathem, Theoretical Studies of Corrosion Inhibition Efficiency of Two New N-Phenyl-Ethylidene-5-Bromo Isatin Derivatives, *Iraqi J. Sci*., 2016, **57**, 1041–1051.
6. V. Brusic, G.S. Frankel, B.M. Rush, A.G. Schrott, C. Jahnes, M.A. Russak and T. Petersen, Corrosion and Passivation of Fe and FeN Films, *J. Electrochem. Soc*., 1992, **139**, 1530. doi: 10.1149/1.2069450
7. Y.H. Lee, S.J. Lee, J.W. Park and H.J. Kim, Synthesis and properties of flexible polyester with urethane polyol for automotive pre-coated metals, *J. Adhes. Sci. Technol*., 2016, **30**, no. 14,1537–1554. doi: 10.1080/01694243.2016.1150673
8. M. Taha, N.H. Ismail, S. Imran, M.Q. Bin Rokei, S.M. Saad and K.M. Khan, Synthesis of new oxadiazole derivatives as α-glucosidase inhibitors, *Bioorg. Med. Chem*., 2015, **23**, no. 15, 4155–4162. doi: 10.1016/j.bmc.2015.06.060
9. H. Tokuhisa, M. Era, T. Tsutsui and S. Saito, Electron drift mobility of oxadiazole derivatives doped in polycarbonate, *Appl. Phys. Lett*., 1995, **66**, 3433. doi: 10.1063/1.113378
10. M.A. Quraishi and D. Jamal, Corrosion inhibition by fatty acid oxadiazoles for oil well steel (N-80) and mild steel, *Mater. Chem. Phys*., 2001, **71**, no. 2, 202–205. doi: 10.1016/S0254-0584(00)00378-3
11. F. Bentiss, M. Traisnel, H. Vezin and M. Lagrenée, Linear resistance model of the inhibition mechanism of steel in HCl by triazole and oxadiazole derivatives: Structure-activity correlations, *Corros. Sci*., 2003, **45**, no. 2, 371–380. doi: 10.1016/S0010-938X(02)00102-6
12. E.A. Yaqo, R.A. Anaee, M.H. Abdulmajeed, I.H.R. Tomi and M.M. Kadhim, Electrochemical, morphological and theoretical studies of an oxadiazole derivative as an anti-corrosive agent for kerosene reservoirs in Iraqi refineries, *Chem. Pap*., 2020, **74**, 1739–1757. doi: 10.1007/s11696-019-01022-2

13. D.M. Gurudatt and K.N. Mohana, Synthesis of new pyridine based 1,3,4-oxadiazole derivatives and their corrosion inhibition performance on mild Steel in 0.5 M hydrochloric acid, *Ind. Eng. Chem. Res*., 2014, **53**, no. 6, 2092–2105. doi: 10.1021/ie402042d
14. R. Palit, N. Saraswat and J. Sahoo, Review on Substituted 1,3,4-Oxadiazole and Its Biological Activities, *Int. Res. J. Pharm*., 2016, **7**, no. 2, 1–7. doi: 10.7897/2230-8407.07212
15. Y. Abboud, A. Abourriche, T. Saffaj, M. Berrada, M. Charrouf, A. Bennamara, A. Cherqaoui and D. Takky, The inhibition of mild steel corrosion in acidic medium by 2,2'-bis(benzimidazole), *Appl. Surf. Sci*., 2006, **252**, no. 23, 8178–8184. doi: 10.1016/j.apsusc.2005.10.060
16. K.A. Al-Saadie, H.A. Abas and H.A.Y. Almashhdani, Corrosion Protection of Iron Alloy Using *Peganum harmala* Extract as Inhibitor in Acidic Solution, *Mater. Sci. Appl*., 2015, **6**, no. 11, 1061–1070. doi: 10.4236/msa.2015.611105
17. E.E. Ebenso, D.A. Isabirye and N.O. Eddy, Adsorption and quantum chemical studies on the inhibition potentials of some thiosemicarbazides for the corrosion of mild steel in acidic medium, *Int. J. Mol. Sci*., 2010, **11**, no. 6, 2473–2498. doi: 10.3390/ijms11062473
18. A.W. Salman, Synthesis and characterization of 1-benzylbenzimidazole complexes with some transition metal salt, *Aust. J. Basic Appl. Sci*., 2015, 9, no. 35, 251–255.
19. M.J. Frisch, G.W. Trucks and H.B. Schlegel, GAUSSIAN 09, Gaussian, Inc., Wallingford, CT, 2009.
20. H. Hejaz, R. Karaman and M. Khamis, Computer-assisted design for paracetamol masking bitter taste prodrugs, *J. Mol. Model*., 2012, **18**, 103–114. doi: 10.1007/s00894-011-1040-5
21. S.H. Kazemi, H. Eshtiagh-Hosseini, M. Izadyar and M. Mirzaei, Computational study of the intramolecular proton transfer between 6-hydroxypicolinic acid tautomeric forms and intermolecular hydrogen bonding in their dimers, *Phys. Chem. Res*., 2013, **1**, 117–125. doi: 10.22036/PCR.2013.3102
22. J.N. Murrell and K.J. Laidler, Symmetries of activated complexes, *Trans. Faraday Soc*., 1968, **64**, 371–377. doi: 10.1039/TF9686400371
23. R.M. Issa, M.K. Awad and F.M. Atlam, Quantum chemical studies on the inhibition of corrosion of copper surface by substituted uracils, *Appl. Surf. Sci*., 2008, **255**, no. 5, 2433–2441. doi: 10.1016/J.APSUSC.2008.07.155
24. B.S. Maluckov, The catalytic role of *Acidithiobacillus ferrooxidans* for metals extraction from mining - metallurgical resource, *Biodiversity Int J*., 2017, **1**, no. 3,109–119. doi: 10.15406/bij.2017.01.00017
25. A. Allouche, Gabedit - A Graphical User Interface for Computational Chemistry Softwares, *J. Comput. Chem*., 2012, **32**, no. 1, 174–182. doi: 10.1002/jcc.21600
26. H.M. Berman, J. Westbrook, Z. Feng, G. Gilliland, T.N. Bhat, H. Weissig, I.N. Shindyalov and P.E. Bourne, The Protein Data Bank, *Nucleic Acids Res*., 2000, **28**, no. 1, 235–242. doi: 10.1093/nar/28.1.235

27. M.M. Kadhim and R.M. Kubba, Theoretical Investigation on Reaction Pathway, Biological Activity, Toxicity and NLO Properties of Diclofenac Drug and Its Ionic Carriers, *Iraqi J. Sci*., 2020, **61**, no. 5, 936–951. doi: 10.24996/ijs.2020.61.5.1
28. A.W. Salman, R.A. Haque, M.M. Kadhim, F.P. Malan and P. Ramasami, Novel triazine-functionalized tetra-imidazolium hexafluorophosphate salt: Synthesis, crystal structure and DFT study, *J. Mol. Struct*., 2019, **1198**, 126902. doi: 10.1016/j.molstruc.2019.126902
29. E.A. Yaqo, R.A. Anaee, H. Abdulmajeed, I. Hameed, R. Tomi and M.M. Kadhim, Electrochemical, morphological and theoretical studies of an oxadiazole derivative as an anti-corrosive agent for kerosene reservoirs in Iraqi refineries, *Chem. Pap*., 2020, **74**, 1739–1757. doi: 10.1007/s11696-019-01022-2
30. R.S. Hatam, S.I. Muslim, R.A. Kadhim, M.M. Kadhim and M. Zaid, Optical properties of different organic compounds: experimental and theoretical studies, *Int. J. Pharm. Res*., 2020, **12**, 798–806.
31. A.A. Khadom, M.M. Kadhim, R.A. Anaee, H.B. Mahood, M.S. Mahdia and A.W. Salman, Theoritical evaluation of *Citrus Aurantium* leaf extract as green inhibitor for chemical and biological corrosion of mild steel in acidic solution: Statistical, molecular dynamics, docking, and quantum mechanics study, *J. Mol. Liq*., 2021, **343**, 116978. doi: 10.1016/J.MOLLIQ.2021.116978
32. D. Hussain, A. Rheima, S. Jaber and M. Kadhim, Cadmium Ions Pollution Treatments in Aqueous Solution Using Electrochemically Synthesized Gamma Aluminum Oxide Nanoparticles with DFT study, *Egypt. J. Chem*., 2020, **63**, no. 2, 417–424. doi: 10.21608/ejchem.2019.16882.2026
33. E.A. Yaqo, R.A. Anaee, M.H. Abdulmajeed, I.H.R. Tomi and M.M. Kadhim, Aminotriazole Derivative as Anti-Corrosion Material for Iraqi Kerosene Tanks: Electrochemical, Computational and the Surface Study, *ChemistrySelect*, 2019, **4**, no. 34, 9883–9892. doi: 10.1002/slct.201902398
34. R.A. Anaee, I.H.R. Tomi, M.H. Abdulmajeed, S.A. Naser and M.M. Kathem, Expired Etoricoxib as a corrosion inhibitor for steel in acidic solution, *J. Mol. Liq*., 2019, **279**, 594–602. doi: 10.1016/j.molliq.2019.01.169
35. H.M. Berman, J. Westbrook, Z. Feng, G. Gilliland, T.N. Bhat, H. Weissig, I.N. Shindyalov and P.E. Bourne, The Protein Data Bank, *Nucleic Acids Res*., 2000, **28**, no. 1, 235–242. doi: 10.1093/nar/28.1.235
36. A. Allouche, Gabedit - A Graphical User Interface for Computational Chemistry Softwares, *J. Comput. Chem*., 2012, **32**, no. 1, 174–182. doi: 10.1002/jcc.21600
37. H. Chermette, Chemical reactivity indexes in density functional theory, *J. Comput. Chem*., 1999, **20**, 129–154.
38. R.M. Kubba and M.M. Khathem, Theoretical Studies of Corrosion Inhibition Efficiency of Two New N-Phenyl-Ethylidene-5-Bromo Isatin Derivatives, *Iraqi J. Sci*., 2016, **57**, 1041–1051.

39. E.A. Yaqo, R.A. Anaee, M.H. Abdulmajeed, I.H.R. Tomi and M.M. Kadhim, Aminotriazole Derivative as Anti-Corrosion Material for Iraqi Kerosene Tanks: Electrochemical, Computational and the Surface Study, *ChemistrySelect*, 2019, **4**, no. 34, 9883–9892. doi: 10.1002/slct.201902398
40. M.M Kadhim, A.W. Salman, A.M. Zarzoor and W.R. Kadhum, Inhibition of SARS-CoV-2 reproduction using Boswellia carterii: A theoretical study, *J. Mol. Liq*., 2021, **337**, 116440. doi: 10.1016/j.molliq.2021.116440
41. E.A. Yaqo, R.A. Anaee, H. Abdulmajeed, I. Hameed, R. Tomi and M.M. Kadhim, Electrochemical, morphological and theoretical studies of an oxadiazole derivative as an anti-corrosive agent for kerosene reservoirs in Iraqi refineries, *Chem. Pap*., 2020, **74**, 1739–1757. doi: 10.1007/s11696-019-01022-2
42. F. Kandemirli and S. Sagdinc, Theoretical study of corrosion inhibition of amides and thiosemicarbazones, *Corros. Sci*., 2007, **49**, no. 5, 2118–2130. doi: 10.1016/j.corsci.2006.10.026
43. H. Wang, L.K. Ju, H. Castaneda, G. Cheng and B.Z. Newby, Corrosion of carbon steel C1010 in the presence of iron oxidizing bacteria *Acidithiobacillus ferrooxidans*, *Corros. Sci*., 2014, **89**, 250–257.
44. H. Li, K.S. Leung, P.J. Ballester and M.H. Wong, Istar: A web platform for large-scale protein-ligand docking, *PLoS One*, 2014, **9**, no. 1. doi: 10.1371/journal.pone.0085678

♦ ♦ ♦